scientific reports

Check for updates

OPEN

High performance double perovskites of $Cs_2InAgBr_6$ and $Cs_2InAgCl_6$ structural electronic optical and thermoelectric properties for next generation photovoltaics

M. Fatmi[1], K. Bouferrache[1,2], M. A. Ghebouli[1,3], B. Ghebouli[4], Faisal Katib Alanazi[5]✉, Munirah D. Albaqami[6], Saikh Mohammad[6] & A. Benali[7]

First-principles calculations carried out using the full potential linearized augmented planewave (FPLAPW) method as implemented in the Wien2K code indicate that the ground state volume of $Cs_2AgInBr_6$ and $Cs_2AgInCl_6$ is 2400 (a.u)^3 and 2050 (a.u)^3, which corresponds to a unit cell energy minimum of − 84,842.919545 Ryd and − 59,101.325763 Ryd. The negative formation energy, Goldschmidt tolerance factor closer to unity and octahedral factor greater than 0.41justify their thermodynamic and structural stability of our investigated double perovskites. The reported lattice constant, ground state energy, bulk modulus and its pressure derivative are closer to their available experimental and theoretical data. Optical analysis reveals high absorption in the visible to ultraviolet range, along with enhanced dielectric constants and optical conductivity. Cs_2AgInX_6(X = Cl, Br) double perovskites are promising candidates for solar cells, thermoelectric devices, and energy harvesting applications due to their tunable band gap, high optical absorption, and enhanced thermoelectric performance.

Keywords Ab-initio, DFT, Structural characterization, Electronic properties, Thermoelectric, Optic

The double perovskite structure with a basic formula $A_2B'B''X_6$ is known as ferroelectric, ferromagnetic and multiferroic materials[1,2]. The choice of the double perovskites elements is such that A is organic cation with a large ionic radius to stabilize the crystal structure, B' and B" are monovalent and trivalent elements and X represents a halide ion. The rare metal (B′ = In) and noble-metal (B″ = Ag) cations alternate along the three crystallographic axes, forming the rock-salt ordering. Double perovskite has improved chemical compatibility and electrical conductivity, so, it can be widely used in photocatalytic and photovoltaic applications. Cs_2AgInX_6(X = Cl, Br) double perovskites materials have potential applications in lighting and high-energy ray detection. This type of perovskite belongs to the $Fm\bar{3}m$(no. 225) space group and the atomistic model consists of In (Cl_6, Br_6) and Ag(Cl_6, Br_6) octahedral which alternate in a rock-salt face-centered cubic structure along the [100], [010], and [001] directions. $Cs_2AgInCl_6$ exhibits white coloration, low photoluminescence emission energy and reveal the suitability for photovoltaic applications[3,4]. Cs_2InAgX_6(X = F, Br, Cl, I) were studied as candidate materials for photovoltaic cells (PVC) using the density functional theory (DFT) methods as implemented in the Quantum Espresso as[5]. The 500 nm and 1000 nm thick films of $Cs_2AgInBr_6$ include Cs_2AgBr_3, $Cs_3In_2Br_9$, AgBr, and

[1]Research Unit on Emerging Materials (RUEM), University Ferhat Abbas of Setif 1, 19000 Setif, Algeria. [2]Department of Physics, Faculty of Science, University of M'sila University Pole, Road Bourdj Bou Arreiridj, 28000 M'sila, Algeria. [3]Department of Chemistry, Faculty of Sciences, University of M'sila University Pole, Road Bourdj Bou Arreiridj, 28000 M'sila, Algeria. [4]Laboratory of Studies Surfaces and Interfaces of Solids Materials, Department of Physics, Faculty of Science, University Ferhat Abbas of Setif 1, 19000 Sétif, Algeria. [5]Department of Physics, College of Sciences, Northern Border University, 73222 Arar, Saudi Arabia. [6]Department of Chemistry, College of Science, King Saud University, 11451 Riyadh, Saudi Arabia. [7]CFisUC, Physics Department, University of Coimbra, Rue Larga, 3004-516 Coimbra, Portugal. ✉email: Faisal.katib.al@gmail.com

$InBr_3$, indicating a partial reaction between CsBr and AgBr and $InBr_3$ during deposition[6]. Other promising double perovskites are recommendable for use as active layers in PVCs such as $Cs_2InSbCl_6$, $Rb_2AgInBr_6$, and $Rb_2CuInCl_6$. Additionally, the band gap of these materials is sensitive to the In(Ag)-(Cl, Br)bond lengths. Cs_2AgInX_6 (X = Cl, Br) double perovskites are candidates as environmentally friendly alternatives[7–10] and they are applied in optoelectronic devices, such as LEDs[10] and solar cells[11–13]. The work of Ying Liu et al.[14], provides a comprehensive characterization of $Cs_2AgInCl_6$ in both bulk crystal and nanocrystal forms, detailing their synthesis methods, intrinsic optical properties, and tunable photoluminescence characteristics. Research by others has demonstrated that $Cs_2AgInCl_6$ possesses advantageous thermoelectric properties, including low lattice thermal conductivity, reduced group velocity, significant phonon scattering, and high Seebeck coefficient values[15]. In the general double perovskite structure, $A_2B'B''X_6$, studies have shown that B-X and B′-X bond lengths exhibit high sensitivity to the computational functionals employed, with the electronic band structure specifically the valence band maximum and conduction band minimum showing an almost linear dependence on these bond lengths[16]. The Cs_2AgInX_6 family (X = Cl, Br, F, I) demonstrates remarkable multifunctional capabilities, including thermoelectric energy conversion, low optical reflectivity, high absorption coefficients, and substantial optical conductivity across visible and UV spectral regions, making them particularly promising for optoelectronic applications[17,18]. Our present work offers a comprehensive investigation of Cs_2AgInX_6 (X = Cl, Br) double perovskites using both GGA and mBJ-GGA functionals, encompassing geometric analysis, structural characterization, and assessment of mechanical, thermodynamic, and dynamic stability, alongside detailed optoelectronic and thermoelectric property evaluations. Our calculations reveal that these compounds exhibit direct band gaps within the visible spectrum, an ideal characteristic for thin-film photovoltaic applications. These double perovskites incorporate mono valent Ag^{+} and trivalent In^{3+} cations, which contribute to their fascinating intrinsic optical behaviors, including self-trapped exciton emission (STE) and element-induced photoluminescence properties that have attracted significant attention in optoelectronic research. The orbital mismatch between Ag (4d) and In (5 s) states generates the direct band gap in these A_2AgInX_6 (X = Cl, Br) materials, further supporting their potential application in solar cell technologies.

Computational methodology

All calculations were performed using the full potential linearized augmented plane wave (FPLAPW) method implemented in the Wien2K code[19]. This approach divides the unit cell into muffin tin (MT) spheres surrounding atoms and an interstitial region. Within each MT sphere, wave functions are represented as atomic-like spherical harmonic radial functions. Basis set convergence was ensured using a cutoff parameter RMTKmax = 7.5, where Kmax represents the largest reciprocal space vector magnitude and RMT the smallest atomic sphere radius. Table 1 lists the specific RMT values for Cs, Ag, In, Cl, and Br atoms in Cs2AgInCl6 and Cs2AgInBr6, carefully selected to prevent charge leakage. Self-consistency was achieved using a 1000 k-point mesh with convergence criteria of 0.0001 Ry for total energy and 0.001e for total charge. For electronic structure calculations, a denser 21×21×21 k-point grid was employed for Brillouin zone integration. The Perdew-Burke-Ernzerhof generalized gradient approximation (PBE-GGA) functional[20] was used for structural optimization of Cs2AgInX6 (X = Cl, Br). For more accurate electronic, optical, and thermoelectric properties, we employed the modified Becke-Johnson exchange potential (mBJ-GGA)[21]. Transport properties were calculated by solving the semi-classical Boltzmann transport equation using the BoltzTrap code.

Results and discussion

Structural analysis

The compounds Cs_2AgInX_6 (X = Cl, Br) crystallize in the cubic double perovskite structure with space group $Fm\bar{3}m$(no. 225), each unit cell containing 10 atoms as illustrated in Fig. 1. The unit cell energy optimization plots for these compounds calculated using the GGA approximation (Fig. 2). As the unit cell volume increases to reach the ground state values of 2400 (a.u)^3 for $Cs_2AgInBr_6$ and 2050 (a.u)^3 for $Cs_2AgInCl_6$, the corresponding unit cell energies decrease to their minimum values of −84842.919545 Ryd and −59101.325763 Ryd, respectively. These optimized structures represent the most stable configurations and serve as the foundation for all subsequent structural parameter calculations in our first-principles approach. The optimization results were validated using the Birch-Murnaghan equation of state[22], which yielded the lattice constant (a_0), ground state energy (E_0), bulk modulus (B_0), and its pressure derivative as presented in Table 2. The calculated ground state parameters show excellent agreement with available experimental data[23] and previously reported theoretical values[5,15]. To evaluate the thermodynamic stability of Cs_2AgInX_6 (X = Cl, Br), we calculated the formation energy using the equation shown in Table 2. This calculation helps determine whether the formation reaction is spontaneous, thereby confirming the compounds' thermodynamic stability. The bulk formation energy in unit cell of 10 atoms is given by[18]:

	$R_{MT}xK_{max}$	R_{MT} (Cs)	R_{MT} (Ag)	R_{MT} (In)	R_{MT} (X)	k-point
$Cs_2InAgBr_6$	9	2.50	2.50	2.50	2.50	1000
$Cs_2InAgCl_6$	9	2.50	2.50	2.50	2.24	1000

Table 1. The values of $R_{MT}xK_{max}$, R_{MT} for each component and k-points for Cs_2InAgX_6(X = Br, Cl). (k-point = 10,000) for optical and thermoelectric properties.

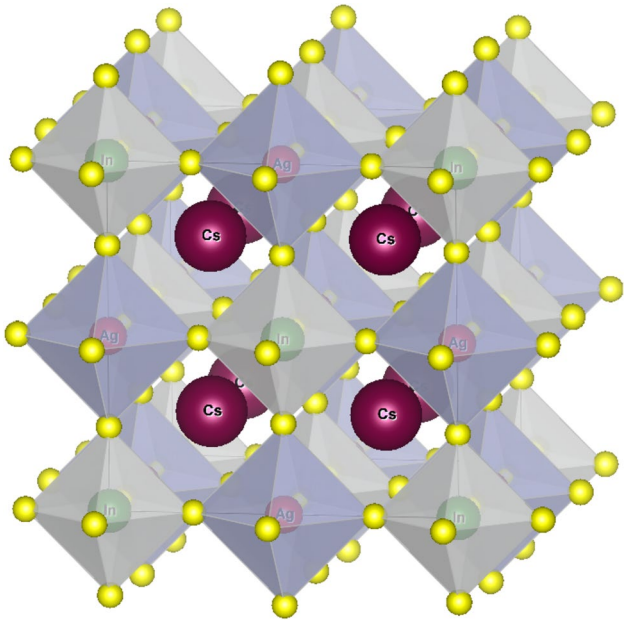

Fig. 1. Schematic crystal structure ofCs_2InAgX_6(X = Br, Cl), Cs cation is located at the middle of the unit cell. Ag and In ions are located alternately in the center of the CsX_6 octahedral. The X anion takes the faces of every unit cell.

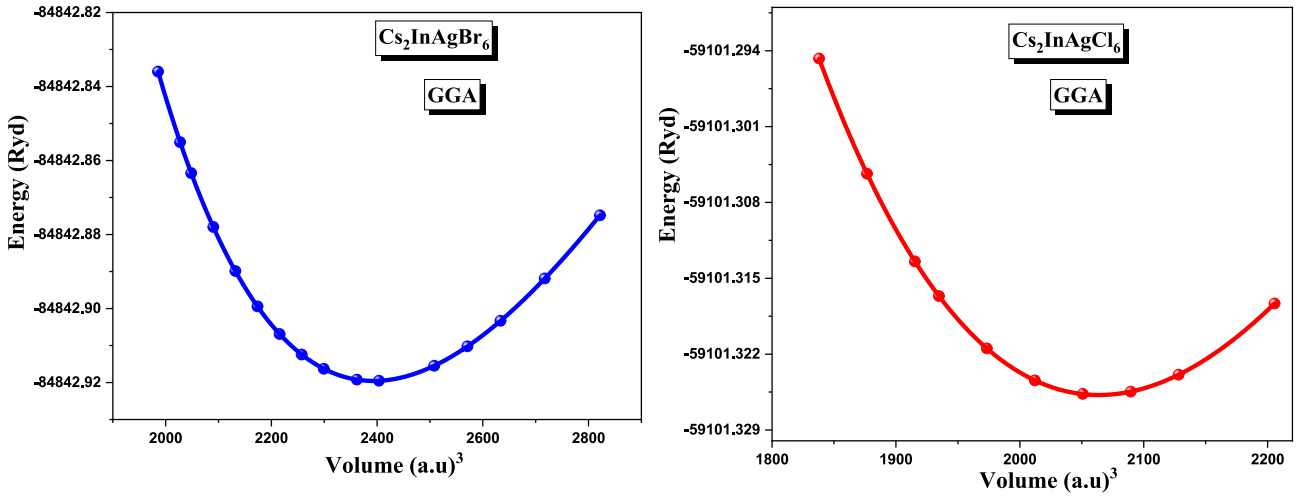

Fig. 2. Unit cell energy optimization plots forCs_2InAgX_6(X = Br, Cl) using GGA approximation.

	a_0 (Å)	B_0 (GPa)	B_0'	ΔE_f (Ry)	t-factor	μ-factor
$Cs_2InAgBr_6$	11.23 10.74[5]	24.10 23.46[15]	5.179 5.00[15]	−84,842.919545 −84,842.919131[15]	0.92 0.92[15]	0.49
$Cs_2InAgCl_6$	10.6947 11.07[5] Exp. 10.478[23]	29.1629 29.12[15]	5.131 4.90[15]	−59,101.325763 59,101.388593[15]	0.937 0.93[15]	0.53

Table 2. Optimized lattice constant, bulk modulus and its pressure derivative and formation energy ΔE_f for Cs_2InAgX_6(X = Br, Cl).

$$\Delta E_f(Cs_2AgInX_6) = \frac{1}{10}\left[E_{tot}(Cs_2AgInX_6) - 2E_s(Cs) - E_s(Ag) - E_s(In) - 6E_s(X)\right]$$

The energy of the Cs, Ag, In and X atoms in this context is denoted E_s(Cs), E_s(Ag), E_s(In) and E_s(X). The Cs_2AgInX_6(X=Cl, Br) unit cell's total energy is represented by E_{tot} (Cs_2AgInX_6).

The negative ΔE_f values justify the thermodynamic stability of our double perovskites. Goldschmidt tolerance factor t and octahedral factor μare necessary for the knowledge of structural stability. The Goldschmidt tolerance factor closer to unity and octahedral factor greater to 0.41 for Cs_2AgInX_6(X = Cl, Br) listed in Table 2, translate their structural stability. The Ag and Inions are located in the center of the CsX_6 octahedral. The Ag–X (In-X) bond length in the same octahedral unit is $d_{Ag\text{-}Cl}$ = 2.77392 Å, $d_{In\text{-}Cl}$ = 2.57362 Å and $d_{Cs\text{-}Cl}$ = 3.78261 Å ($d_{Ag\text{-}Br}$ = 2.87672 Å, $d_{In\text{-}Br}$ = 2.74198 Å and $d_{Cs\text{-}Br}$ = 3.97359 Å). Small bond lengths in a material result in a low lattice constant. The bond length $d_{Ag\text{-}Cl}$ and $d_{In\text{-}Cl}$ are in good concordance with their theoretical values2.76 Å and 2.57 Å reported in the literature[9].

Electronic structure characteristics

Fig. 3 shows the electronic band structures of Cs_2AgInX_6 (X = Cl, Br) calculated along the high-symmetry points (W, L, Γ, X, K) in the Brillouin zone using different functionals: GGA, GGA with spin-orbit coupling (SOC), mBJ-GGA, and mBJ-GGA with SOC. Our calculations reveal direct band gaps at the Γ point of 1.049 eV for $Cs_2InAgCl_6$ and 0.218 eV for $Cs_2InAgBr_6$ using the GGA functional. These values increase significantly to 1.68 eV and 2.61 eV, respectively, when employing the more accurate mBJ-GGA functional. To assess the effect of spin-orbit coupling, additional calculations using GGA-SOC and mBJ-GGA-SOC functionals were performed. The results, summarized in Table 3, show a slight reduction in the band gap values upon inclusion of SOC. For example, the mBJ-GGA band gap of $Cs_2AgInBr_6$ decreases slightly from 1.75 eV to 1.68 eV, while $Cs_2AgInCl_6$ shows a minor decrease from 2.64 to 2.61 eV. These findings indicate that although SOC slightly modifies the electronic structure, the overall qualitative features remain unchanged. Despite these improvements, both functionals still underestimate the experimental band gap of 3.23 eV reported for $Cs_2InAgCl_6$[24]. We observed that band gap values are highly sensitive to Ag-X and In-X bond lengths, with smaller bond lengths generally corresponding to larger band gaps. The band gap tuning capability through the Ag-In site manipulation makes

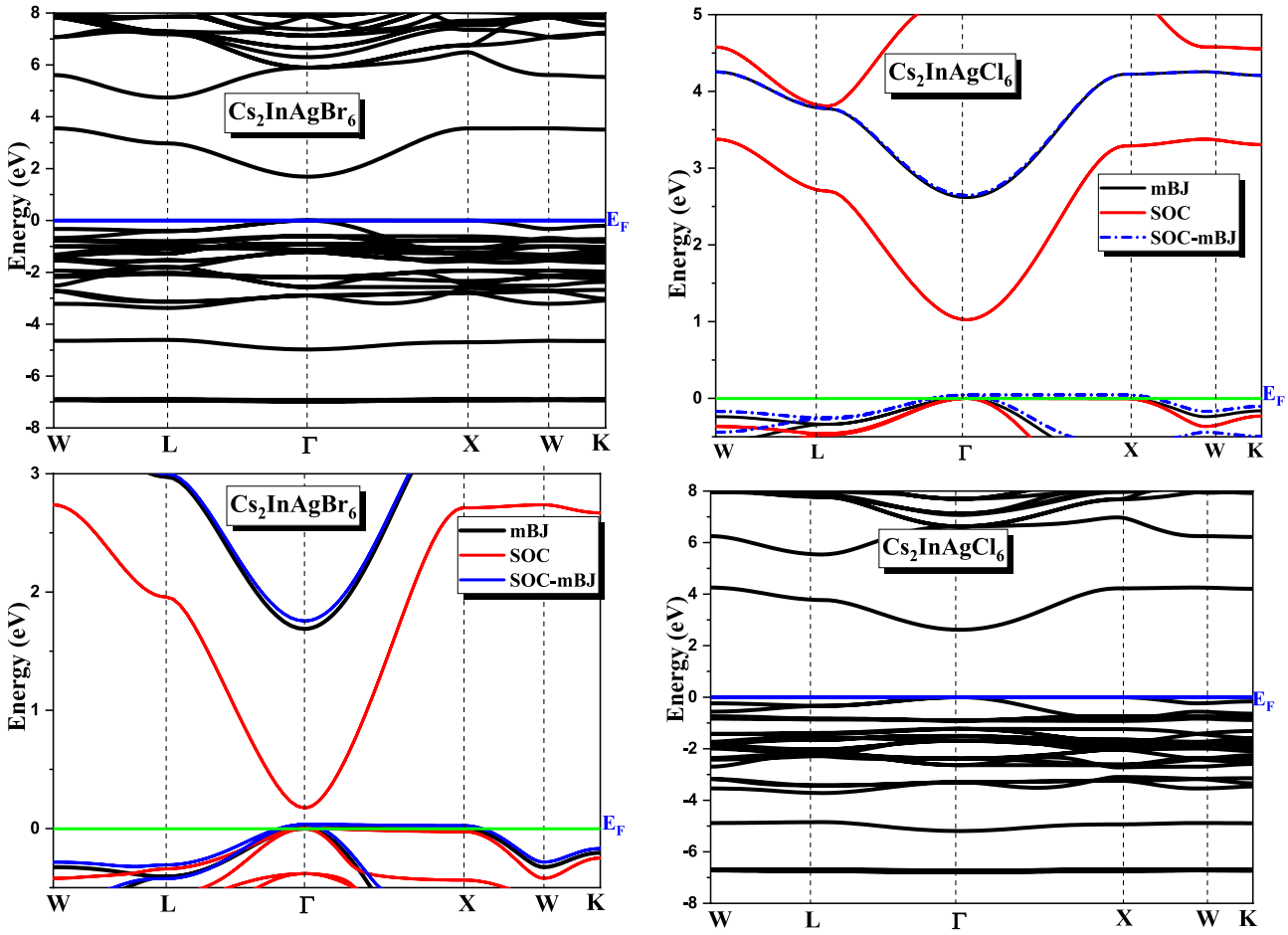

Fig. 3. Electronic band structure of Cs_2AgInX_6(X = Cl, Br) using GGA, GGA with spin–orbit coupling (SOC), mBJ-GGA, and mBJ-GGA with SOC.

	GGA	GGA-mBJ	GGA-SOC	GGA-SOC-mBJ
$Cs_2InAgBr_6$	0.218	1.68 1.83[25] 1.74[2] 1.50[26]	0.174	1.75
$Cs_2InAgCl_6$	1.049	2.61 2.74[25] 3.3[2]exp 2.53[15]	1.025	2.64

Table 3. The band gap of Cs2InAgX6 (X = Br, Cl) using GGA, andGGA-mBJ,GGA-SOC, GGA-SOC-mBJ. Further analysis of the partial density of states (PDOS) using mBJ-GGA calculations.

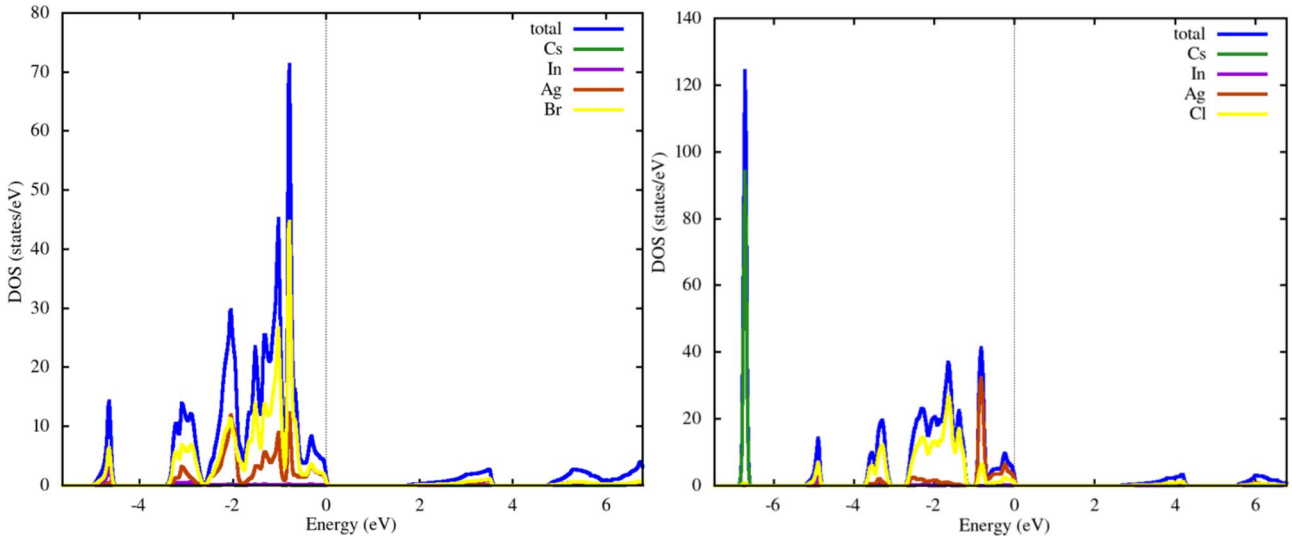

Fig. 4. Partial and total densities of states for $Cs_2AgInBr_6$ and $Cs_2AgInCl_6$.

these materials particularly promising for photovoltaic applications, where an optimal band gap of approximately 1.5 eV is desired for maximum efficiency. Examination of the band dispersion reveals a notably flat first valence band along the Γ point, contrasting with a highly dispersive first conduction band. The partial and total densities of states (Fig. 4) show an empty conduction band bottom, while the upper valence band comprises primarily Br-4p, Cl-3p, and Ag-5s orbitals. At the X point, the conduction band edge exhibits a distinctive split into two bands separated by approximately 2 eV.

Figures 5 and 6 confirms strong hybridization at the valence band maximum between Ag-5s and halide p-orbitals (Cl-3p or Br-4p). With the Fermi level (EF) set at 0 eV, the absence of density of states at EF validates the semiconductor nature of these materials. The valence band predominantly consists of contributions from Ag-4d, Cl-3p, and Br-4p orbitals, with minor contributions from In-5p orbitals.

Optical properties

Figure 7; presents a comprehensive analysis of the optical properties of Cs_2InAgX_6 (X = Br, Cl) double perovskites calculated using the mBJ-GGA functional, including absorption coefficient, energy loss, dielectric function components, refractive index, extinction coefficient, optical conductivity, and reflectivity as functions of photon energy. These cubic double perovskites demonstrate remarkable optical characteristics, particularly their exceptional ultraviolet absorption, low reflectivity, and high conductivity properties that are highly advantageous for photovoltaic applications. The calculated optical properties of Cs_2AgInX_6 (X = Br, Cl) compounds show good agreement with previous experimental studies conducted by Zhou et al.[24] and Luo et al.[23]. The high absorption in the ultraviolet range can be attributed to electronic transitions between Ag-4d and X-np orbitals (where n=3 for chlorine and n=4 for bromine), as confirmed by Liu et al.[14]. The elevated absorption coefficient values (260×10^4 cm^{-1} for $Cs_2AgInCl_6$ and 220×10^4 cm^{-1} for $Cs_2AgInBr_6$) indicate superior performance for solar cell applications, significantly exceeding the typical required values (10^4 cm^{-1}), which allows for the use of very thin layers for effective light absorption[17]. The high dielectric constant values (3.4 for $Cs_2AgInBr_6$ and 2.8 for $Cs_2AgInCl_6$) suggest reduced electron-hole recombination rates, an important characteristic for improving solar cell efficiency as noted by Mehedi Hasan et al.[18]. At higher energies, the real part becomes negative, indicating metallic behavior, while the imaginary component shows elevated values across both visible and ultraviolet regions, corresponding to increased absorption. Additionally, the high optical conductivity values (9000 Ω^{-1} cm^{-1} for $Cs_2AgInCl_6$ and 7000 Ω^{-1} cm^{-1} for $Cs_2AgInBr_6$) reflect the high capacity for electrical charge transport upon exposure to optical radiation, which is crucial for the efficient operation of optoelectronic devices. Moreover, the

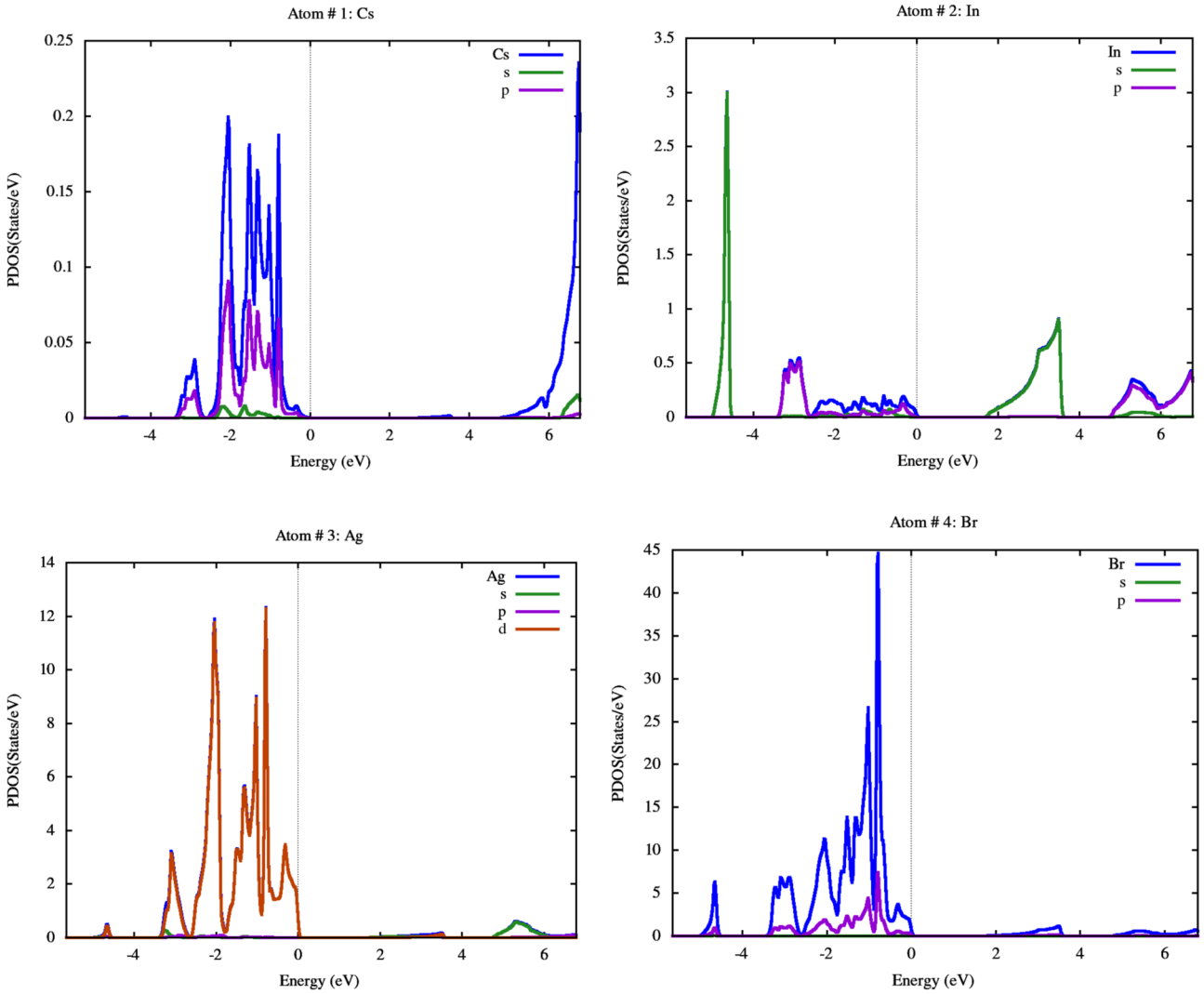

Fig. 5. Partial density of states (PDOS) for $Cs_2InAgBr_6$ using mBJ-GGA calculation.

low reflectivity values (approximately 0.5) indicate that these materials allow a large proportion of light to enter, increasing photon absorption efficiency. Compared to other perovskite materials used in solar cells, Cs_2AgInX_6 (X = Br, Cl) compounds exhibit better thermal and chemical stability[3], alongside their distinguished optical properties, making them a promising choice for the next generation of solar energy applications. Energy loss spectra show negligible loss in the visible region, with maximum losses occurring in the ultraviolet range between 20 and 23 eV. The refractive index exhibits higher values in the visible and ultraviolet ranges due to photon-electron interactions, displaying characteristic oscillatory behavior. When the refractive index falls below unity, superluminal group velocities are theoretically possible. The extinction coefficient, indicating a material's ability to absorb or reflect radiation, shows favorable successive peaks throughout the visible and ultraviolet spectrum. Notably, both materials demonstrate significant photoconductivity in the ultraviolet region, suggesting efficient electron-hole pair generation and charge carrier separation resulting from strong absorption. These favorable optical parameters collectively establish $Cs_2AgInBr_6$ and $Cs_2AgInCl_6$ as promising candidates for solar cell and optoelectronic device applications.

Thermoelectric characteristic

In this study, thermoelectric properties were calculated using the BoltzTraP code[25], which applies semiclassical Boltzmann transport theory under the constant relaxation time approximation (CRTA). The electronic structure was computed with the modified Becke-Johnson (mBJ) potential to improve the accuracy of band gap estimation. A dense k-point mesh of 21×21×21 was employed to ensure convergence of transport coefficients over a temperature range of 300–800 K. The relaxation time (τ) was assumed to be 10^{-14} seconds, consistent with values commonly used in similar halide double perovskite studies (Smith et al., 2021). Fig. 8 presents temperature-dependent thermoelectric parameters calculated with the mBJ-GGA approximation, including Seebeck coefficient, electronic and lattice thermal conductivities, total thermal conductivity, electrical conductivity, and the figure of merit ZT. The calculated Seebeck coefficient reaches values up to 300 μV/K at

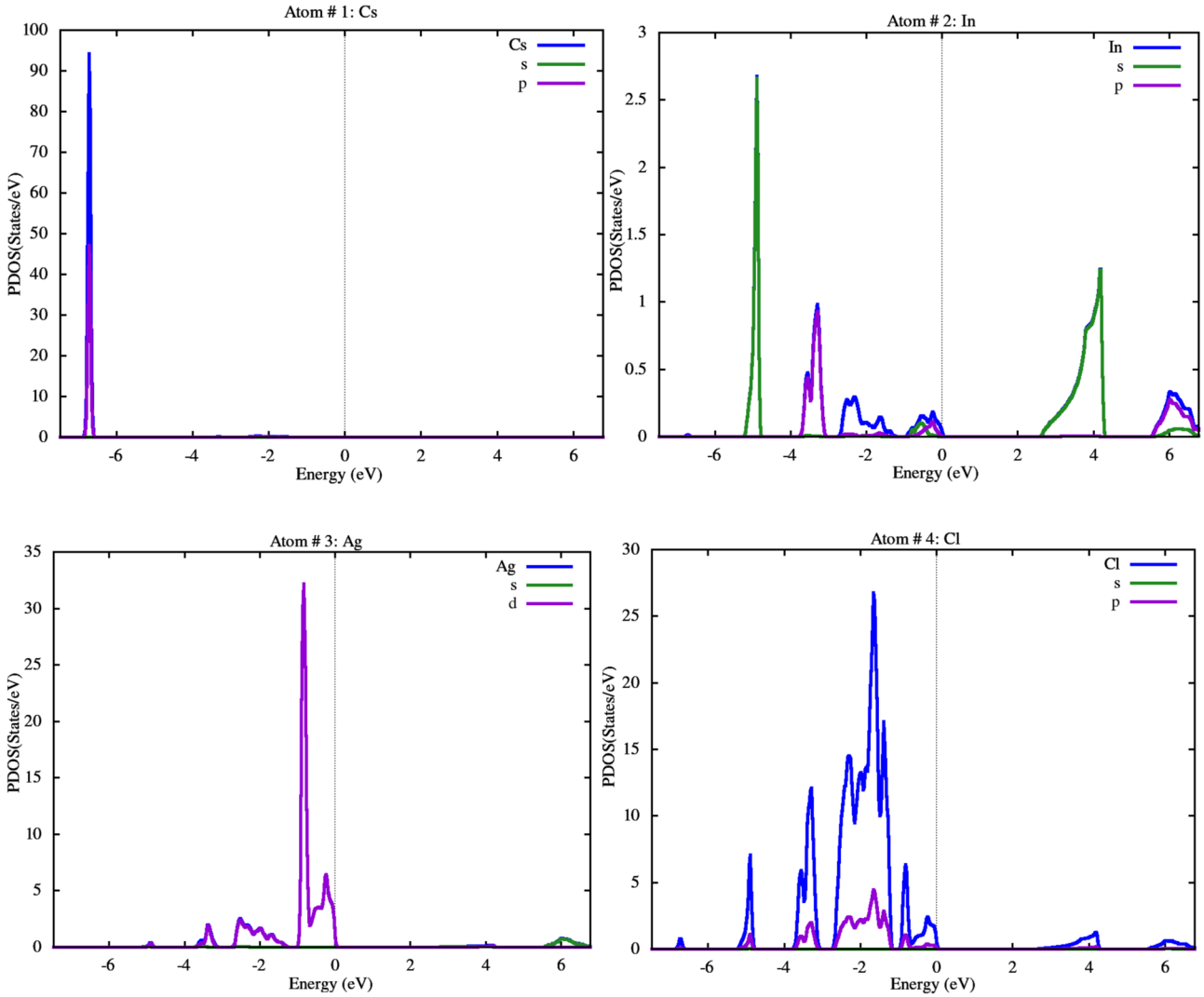

Fig. 6. Partial density of states (PDOS) for $Cs_2InAgCl_6$ using mBJ-GGA calculation.

room temperature, indicating promising thermoelectric performance comparable to previously reported double perovskite materials[27]. The positive Seebeck coefficients (0.68 for $Cs_2AgInBr_6$ and 0.67 for $Cs_2AgInCl_6$ at room temperature) confirm these materials as p-type semiconductors. Thermal transport properties show complementary temperature dependencies, with electronic thermal conductivity increasing monotonically as temperature rises, while lattice thermal conductivity displays the opposite trend, decreasing with temperature elevation. The total thermal conductivity predominantly follows the electronic component's behavior. Electrical conductivity demonstrates a positive correlation with temperature, further validating the semiconducting nature of both double perovskites. Electrical conductivity and electronic thermal conductivity were also evaluated, showing reasonable agreement with experimental and theoretical data from the literature[28]. The thermoelectric efficiency is quantified by the dimensionless figure of merit $ZT = S^2\sigma T/\kappa$, where S represents the Seebeck coefficient, σ the electrical conductivity, T the absolute temperature, and κ the total thermal conductivity.

where; $\kappa = \kappa_e + \kappa_e + k_L$ is the total thermal conductivity, κ_e and κ_e are the electronic thermal conductivities and κ_l is the lattice thermal conductivity.

Since the lattice thermal conductivity κl plays a crucial role in determining ZT, it is important to estimate it accurately. One widely used semi-empirical approach to calculate κl is the Slack[29] a$_2$nd Berman[30] model, which expresses κl as:

$$k_L = A\frac{\overline{M}\theta_D^3\delta}{\gamma^2 T n^{2/3}}$$

γ is the Grüneisen parameter, θ_D is the Debye temperature, and *n* is the number of atoms in the primitive unit cell. Also, $\overline{M}$ and δ^3 are the atoms' average mass in the crystal and the average volume occupied by one atom in the crystal, respectively. Julian[31] provides the following formula for calculating the parameter A.

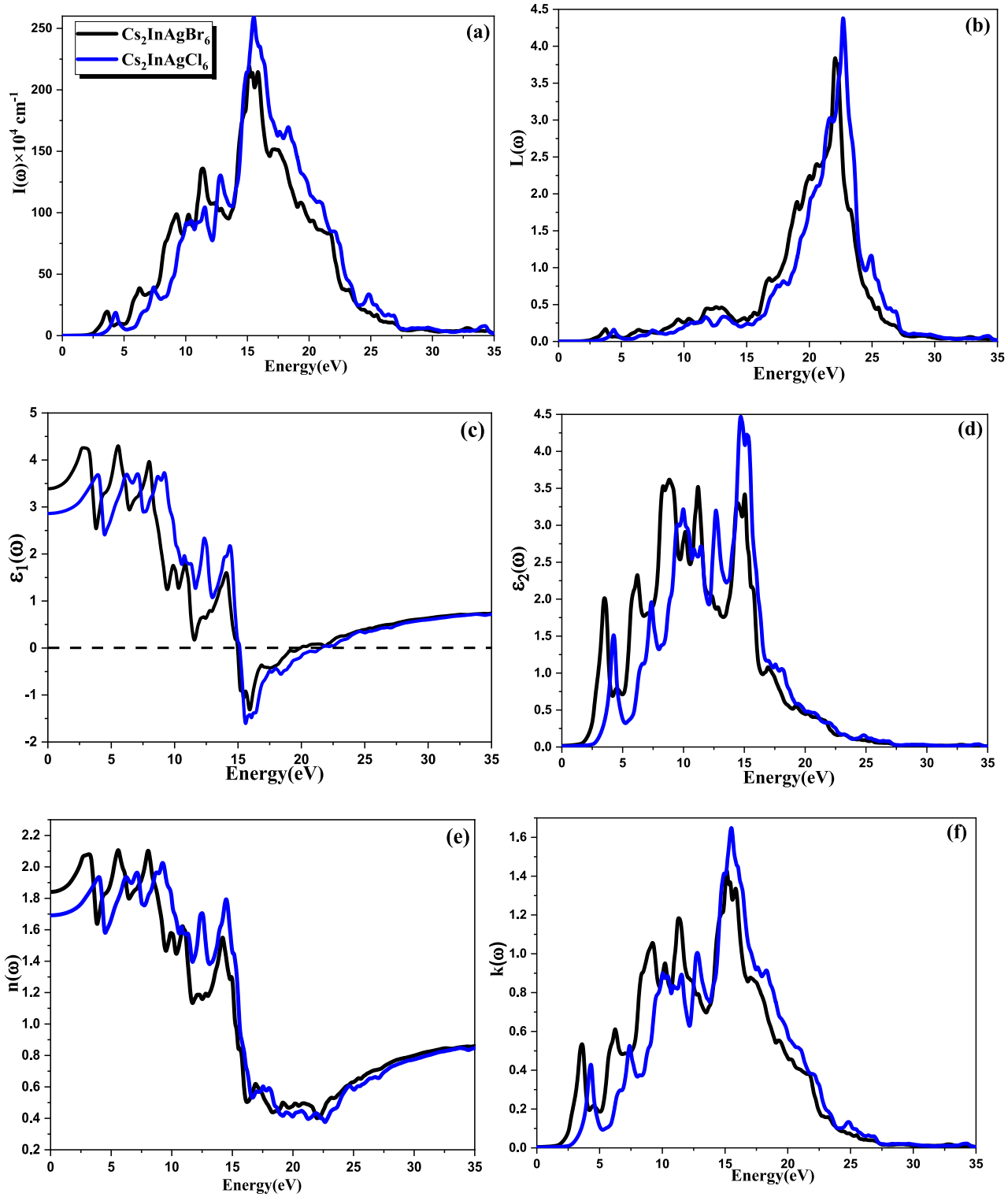

Fig. 7. Absorption coefficient (**a**), energy loss (**b**), real (**c**) and imaginary (**d**) components of the dielectric function, refractive index (**e**), extinction coefficient (**f**) and real optical conductivity (**g**) and reflectivity (**h**) as functions of photon energy for Cs_2InAgX_6(X = Br, Cl) double perovskites using mBJ-GGA.

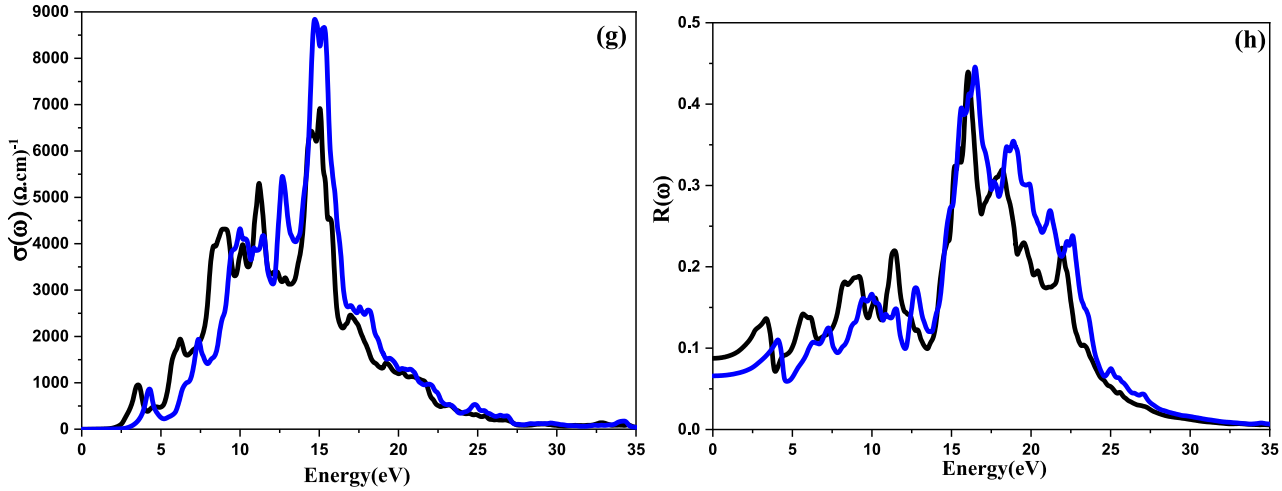

Fig. 7. (continued)

$$A = \frac{2.43 * 10^{-8}}{1 - \frac{0.514}{\gamma} + \frac{0.288}{\gamma^2}}$$

Higher ZT values indicate superior thermoelectric performance. The favorable Seebeck coefficients observed at room temperature suggest promising thermoelectric applications for these environmentally friendly double perovskites. The figure of merit (ZT) was estimated by combining these electronic transport properties with lattice thermal conductivity values reported for similar compounds, suggesting potential for further enhancement via phonon scattering engineering[32]. The relatively flat valence band near the Fermi level contributes to the high Seebeck coefficient, as discussed in previous works on halide perovskites[33]. These results highlight the potential of Cs_2InAgX_6 compounds as efficient thermoelectric materials.

Conclusion

$Cs_2AgInCl_6$ and $Cs_2AgInBr_6$ materials belong to the $Fm\bar{3}m$ space group and consist of $InCl_6$ ($InBr_6$) and $AgCl_6$ ($AgBr_6$) octahedral alternating in a rock-salt face-centered cubic structure. Ag-Cl (Ag-Br), In-Cl (In-Br) and Ag-In bond lengths reduce the direct band gap of $Cs_2AgInCl_6$ and $Cs_2AgInBr_6$ materials to optimal values of 2.61 eV and 1.68 eV, which enable their use in photovoltaic application. The absence of TDOS at the Fermi level and the contribution of Ag-4d, Cl-3p and Br-4p orbitals in the upper valence band reflect the semiconducting character of these double perovskites. $Cs_2AgInCl_6$ and $Cs_2AgInBr_6$ double perovskites provide interesting optical characteristics in the ultraviolet light, such as a greater real component of dielectric function 3.5 and 4.2, high absorption coefficient of $260\times10^4 cm^{-1}$ and $220\times10^4\ cm^{-1}$, lower reflectivity of 0.5, and elevated conductivity of 9000 $\Omega^{-1}cm^{-1}$ and 7000 $\Omega^{-1}cm^{-1}$, then they are effective ultraviolet optical absorbers.

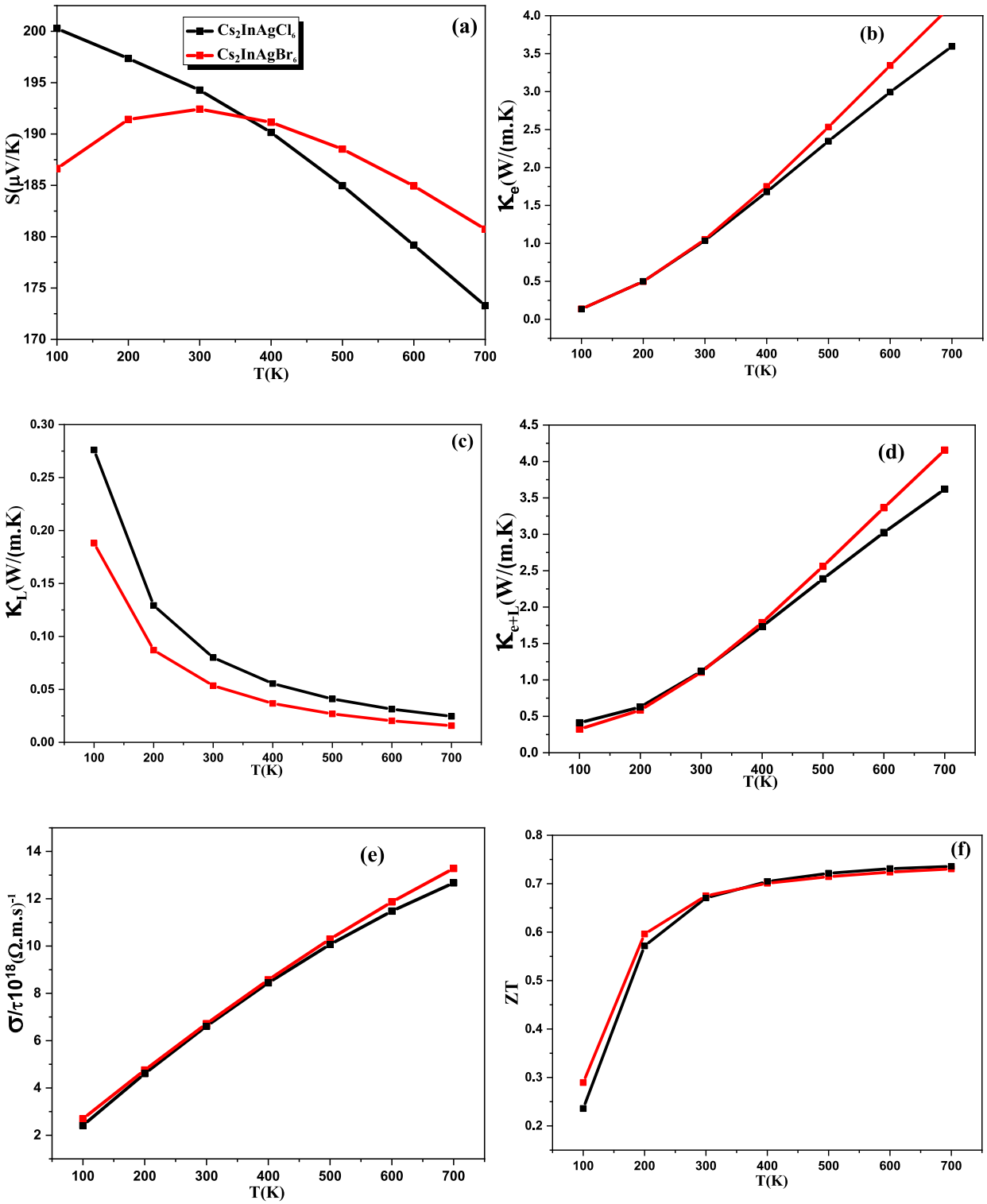

Fig. 8. Computed Seebeck coefficient, electronic thermal conductivity, lattice thermal conductivity, total thermal conductivity, electrical conductivity and the figure of merit ZT as a function of temperature for Cs_2InAgX_6(X = Br, Cl) using mBJ-GGA approximation.

Data availability statement

Data underlying the results presented in this paper are not publicly available at this time but may be obtained from the author (fatmimessaoud@yahoo.fr) upon reasonable request.

Received: 9 April 2025; Accepted: 28 May 2025

Published online: 01 July 2025

References

1. Vasala, S. & Karppinen, M. A2B′ B ″O6 perovskites: A review. *Prog. Solid State Chem.* **43**, 1–36 (2015).
2. Volonakis, M., Filip, A. and Haghighirad, N. S., Wenger, B., Snaith, H. J., and Giustino, F. 2016. *J. Phys. Chem. Lett* **7** 1254–1259.
3. Volonakis, G. et al. $Cs_2InAgCl_6$: A new lead-free halide double perovskite with direct band gap. *J. Phys. Chem. Lett.* **8**, 772–778 (2017).
4. Meng, W. et al. Parity-forbidden transitions and their impact on the optical absorption properties of lead-free metal halide perovskites and double perovskites. *J. Phys. Chem. Lett.* **8**, 2999–3007 (2017).
5. Atarah, S. A. A first-principles study of the mechanical stability and electronic properties of lead-free halide inorganic double perovskites Cs_2InAgX_6 (X= F, Br, Cl, I). *Sci. Dev.* **7**, 17–31 (2023).
6. Liu, Y., Cleveland, I. J., Tran, M. N. & Aydil, E. S. Stability of the halide double perovskite $Cs_2AgInBr_6$. *J. Phys. Chem. Lett.* **14**, 3000–3006 (2023).
7. Luo, J. et al. Efficient and stable emission of warm-white light from lead-free halide double perovskites. *Nature* **563**, 541–545 (2018).
8. Zhou, J. et al. Manipulation of Bi3+/In3+ transmutation and Mn2+-doping effect on the structure and optical properties of double perovskite Cs_2NaBi_1−xInxCl_6. *Adv. Opt. Mater.* **7**, 1801435 (2019).
9. Ning, W. et al. Thermochromic lead-free halide double perovskites. *Adv. Funct. Mater.* **29**, 1807375 (2019).
10. Majher, J. D., Gray, M. B., Strom, T. A. & Woodward, P. M. $Cs_2NaBiCl_6$: Mn2+—a new orange-red halide double perovskite phosphor. *Chem. Mater.* **31**, 1738–1744 (2019).
11. Greul, E., Petrus, M. L., Binek, A., Docampo, P. & Bein, T. Highly stable, phase pure $Cs_2AgBiBr_6$ double perovskite thin films for optoelectronic applications. *J. Mater. Chem. A* **5**, 19972–19981 (2017).
12. Gao, W. et al. High-quality $Cs_2AgBiBr_6$ double perovskite film for lead-free inverted planar heterojunction solar cells with 2.2% efficiency. *ChemPhysChem* **19**, 1696–1700 (2018).
13. Pantaler, M. et al. Hysteresis-free lead-free double-perovskite solar cells by interface engineering. *ACS Energy Lett.* **3**, 1781–1786 (2018).
14. Liu, Y., Nag, A., Manna, L. & Xia, Z. Lead-free double perovskite $Cs_2AgInCl_6$. *Angew. Chem.* **133**, 11696–11707 (2021).
15. Haque, E. & Hossain, M. A. Electronic, phonon transport and thermoelectric properties of $Cs_2InAgCl_6$ from first-principles study. *Comput. Condens. Matter* **19**, e00374 (2019).
16. Ji, Y., Lin, P., Ren, X. & He, L. Geometric and electronic structures of Cs 2 BB′ X 6 double perovskites: The importance of exact exchange. *Phys. Rev. Res.* **6**, 033172 (2024).
17. Tariq, M., Ali, M. A., Laref, A. & Murtaza, G. Anion replacement effect on the physical properties of metal halide double perovskites Cs_2AgInX_6 (X= F, Cl, Br, I). *Solid State Commun.* **314**, 113929 (2020).
18. Hasan, M. M., Sarker, M. A., Islam, M. R. & Islam, M. R. First-principles analysis of the effects of halogen variation on the properties of lead-free novel perovskites $AlGeX_3$ (X= F, Cl, Br, and I). *ACS Omega* **9**, 35301–35312 (2024).
19. Bouferrache, K. et al. Effect of functional on structural, elastic stability, optoelectronic and thermoelectric characteristics of semiconducting MgX2Se4 (X= Lu, Y) spinels. *Bull. Mater. Sci.* **47**, 102 (2024).
20. Ghebouli, B., Ghebouli, M., Fatmi, M. & Ahmed, S. First-principles study of structural, elastic, electronic and lattice dynamic properties of AsxPyN1− x− yB quaternary alloys. *Comput. Mater. Sci.* **48**, 94–100 (2010).
21. Ghebouli, M., Bouferrache, K., Alanazi, F. K., Ghebouli, B. & Fatmi, M. Stability, mechanical, optoelectronic and thermoelectric behaviors of inorganic metal halide double perovskites (Cs2, K2, Rb2) SnCl6: Promising green energy alternatives. *Solid State Commun.* **397**, 115831 (2025).
22. Ghebouli, M., Bouferrache, K., Alanazi, F. K., Ghebouli, B. & Fatmi, M. Computational insights into the stability, mechanical, optoelectronic, and thermoelectric characteristics investigation on lead-based double perovskites of (Cs2, K2, Rb2) PbCl6: Promising candidates for optoelectronic applications. *Adv. Theory Simul.* **8**, 2400938 (2025).
23. Luo, J. et al. $Cs_2AgInCl_6$ double perovskite single crystals: parity forbidden transitions and their application for sensitive and fast UV photodetectors. *ACS Photonics* **5**, 398–405 (2018).
24. Zhou, J. et al. Composition design, optical gap and stability investigations of lead-free halide double perovskite $Cs_2AgInCl_6$. *J. Mater. Chem. A* **5**, 15031–15037 (2017).
25. Madsen, G. and Singh, D. J. 2006. Program title: BoltzTrap Catalogue identifier: ADXU_v1_0 distribution format: tar. gz. *J Reference: Comput. Phys. Commun.* **175**, 67
26. Zhao, X.-G. et al. Cu–In halide perovskite solar absorbers. *J. Am. Chem. Soc.* **139**, 6718–6725 (2017).
27. Gueridi, B., Bouferrache, K., Ghebouli, M. A., Rouabah, F., Slimani, Y., Chihi, T., Fatmi, M., Ghebouli, B., Bouandas, H., Habila, M., Benali, A. Physical properties of rutile-TiO_2 nanoparticles and effect on PVA/SiO2 hybrid films synthesized by sol-gel method. High Energy Density Phys. **52**, 101122 (2024).
28. Su, Y. et al. An investigation on carrier transport behavior of tetragonal halide perovskite: First-principles calculation. *Mater. Sci. Semicond. Process.* **150**, 106836 (2022).
29. Slack, G. A. Nonmetallic crystals with high thermal conductivity. *J. Phys. Chem. Solids* **34**, 321–335 (1973).
30. Hamici, M., Alanazi, F. K., Chihi, T., Fatmi, M. and Ghebouli, M. 2025. Optical, structural, electronic, and population analysis of WO_3–Bi_2O_3 system for emerging and electrical applications. *J. Indian Chem. Soc.* 101729
31. Julian, C. L. Theory of heat conduction in rare-gas crystals. *Phys. Rev.* **137**, A128 (1965).
32. Kumar, A., Muthukumar, P., Sharma, P. & Kumar, E. A. Absorption based solid state hydrogen storage system: A review. *Sustain. Energy Technol. Assess.* **52**, 102204 (2022).
33. Chen, Y., Liu, X., Wang, T. & Zhao, Y. Highly stable inorganic lead halide perovskite toward efficient photovoltaics. *Acc. Chem. Res.* **54**, 3452–3461 (2021).

Acknowledgements

Acknowledgement The authors extend their appreciation to the Deanship of Scientific Research at Northern Border University, Arar, KSA for funding this research work through the project number NBU-FFR-2025-310-13.

Author contributions

Conceptualization: K. Bouferrache, M.A. Ghebouli, B. Ghebouli, Formal analysis: Munirah D. Albaqami, Saikh Mohammad, A. Benali, Validation: M. Fatmi, Faisal Katib Alanazi.

Declarations

Competing interests

The authors declare no competing interests.

Additional information

Correspondence and requests for materials should be addressed to F.K.A.